Self-Optimizing Near and Far-Field MIMO Transmit Waveforms

Sanaz Naderi[®], *Graduate Student Member, IEEE*, Dimitris A. Pados[®], *Senior Member, IEEE*, George Sklivanitis[®], *Member, IEEE*, Elizabeth Serena Bentley, *Member, IEEE*, Joseph Suprenant, and Michael J. Medley, *Senior Member, IEEE*

Abstract—We consider the problem of dynamically optimizing a multiple-input multiple-output (MIMO) wireless waveform in a given potentially heavily utilized fixed frequency band with applications in near-field or far-field autonomous machine-tomachine communications. In particular, we find the transmitter beam weight vector and the pulse code sequence that maximize the signal-to-interference-plus-noise ratio (SINR) at the output of the maximum SINR joint space-time receiver filter. We propose and derive two novel model-based solutions: (a) Disjoint, space first (transmit weight vector) then time (pulse code sequence) waveform optimization and (b) jointly optimal transmit weight vector and pulse code sequence optimization (a mixed integer programming problem.) The proposed formally derived algorithmic solutions are studied in extensive simulations under varying waveform code length, near-field/far-field and spreadspectrum/non-spread-spectrum interference, in light and dense interference scenarios. Our findings highlight the effectiveness of the described methods compared to static conventionally designed MIMO links and the remarkable ability of the joint space-time optimized waveforms to avoid heavy interference.

Index Terms—Autonomous communications, directional networking, interference avoidance, machine-to-machine communications, MIMO, near field communications, space-time waveform design.

I. INTRODUCTION

ELECTROMAGNETIC interference has always been a crucial concern across all generations of wireless communication systems [1]. Today, given the explosive growth in the number of wireless users and the expectation of data transfer rates in the order of hundreds of Mbps, especially for emerging technologies such as machine-to-machine communications [2], [3], [4], broadband Internet of Things [5], millimeter

Manuscript received 1 April 2023; revised 20 August 2023; accepted 5 October 2023. Date of publication 19 April 2024; date of current version 29 May 2024. This work was supported in part by the National Science Foundation under Grant CNS-1753406, Grant CNS-2117822, Grant EEC-2133516, and Grant ECCS-2030234; and in part by the Air Force Research Laboratory under Grant FA8750-21-1-0500. (Corresponding author: Sanaz Naderi.)

Sanaz Naderi, Dimitris A. Pados, and George Sklivanitis are with the Center for Connected Autonomy and AI and the Department of Electrical Engineering and Computer Science, Florida Atlantic University, Boca Raton, FL 33431 USA (e-mail: snaderi2021@fau.edu; dpados@fau.edu; gsklivanitis@fau.edu).

Elizabeth Serena Bentley, Joseph Suprenant, and Michael J. Medley are with the Air Force Research Laboratory, Information Directorate (AFRL/RI), Rome, NY 13441 USA (e-mail: elizabeth.bentley.3@us.af.mil; joseph.suprenant@us.af.mil; michael.medley@us.af.mil).

Color versions of one or more figures in this article are available at https://doi.org/10.1109/JSAC.2024.3389123.

Digital Object Identifier 10.1109/JSAC.2024.3389123

wave (mm-wave) robotics [4], wireless security [6], [7], [8], ultra-reliable low latency (URLLC) networks [9], enhanced mobile broadband (eMBB) [10], massive machine-type communications (mMTC) [11], etc., interference management and avoidance become increasingly challenging and attract significant attention [1], [12], [13]. A method to deal with interference concerns is interference avoidance via dynamic waveform design at a fine time scale [14], [15], [16], [17], [18] where a finite sequence of repeated pulses (say, square-root-raised cosines (SRRC)) that span the entire continuum of the device-accessible spectrum is code optimized over a finite pulse-modulation alphabet to maximize the signal-to-interference-plus-noise ratio (SINR) at the output of the max-SINR filter at the intended receiving node [19], [20].

Multiple-input multiple-output (MIMO) technology is by now well understood as a crucial component in 5G and beyond communications [21], [22], [23]. MIMO systems increase channel capacity, reduce bit-error-rate (BER) and power consumption for a fixed channel data rate, and present unique interference avoidance opportunities in the form of directional transmission and space-time precoding and directional reception and space-time filtering that exploit the product of the spatial and time domain degrees of freedom (DOF) [24], [25]. There are on-going efforts in the literature to deal with interference dilemmas in the time domain by deploying distributed deep learning models, such as [26] that considered 5G/broadband IoT networks. In [20], a similar IoT network was considered but instead of deep learning, an optimal adaptive sparse waveform design algorithm was proposed which adjusts digitally the shape of the waveforms in such a way that the SINR at the output of the maximum-SINR linear filter at the receiver was maximized. A mechanism for interference management in MIMO systems was proposed in [27] where the authors focused on the energy loss problem at downlink transmitters and combined power water-filling algorithms with linear precoding to mitigate interference effects between users. In [19], the problem of directional space-time waveform design for proactive interference avoidance in narrowband far-field MIMO systems was considered. The authors proposed to establish communication between an intended transmitter-receiver pair by a jointly optimized pulse code sequence and signal angle-of-arrival (AoA) that maximized the maximum achievable pre-detection SINR at the output of the max-SINR receiver filter. Gaussian MIMO channels under total transmit and interference power constraints

0733-8716 © 2024 IEEE. Personal use is permitted, but republication/redistribution requires IEEE permission. See https://www.ieee.org/publications/rights/index.html for more information.

were considered in [28] and [29] where the authors obtained by the Karush-Kuhn-Tucker (KKT) approach a closed-form solution for the optimal transmit covariance matrix. The work in [30] focused on the weighted sum-rate maximization problem for wireless cellular MIMO networks with full-duplex base stations and half-duplex mobile devices. In this context, an interference shaping algorithm was developed to decompose the sum-rate problem into independent sub-problems solved locally for each base station under varying constraints. A MIMO relay system was considered in [31] where multiple transmitter and receiver pairs communicate at once through a single relay node. For this system model, the authors proposed a new algorithm that jointly optimized the relay precoding matrix and the receiver matrices based on the minimum sum mean-squared error criterion.

In this paper, we address for the first time in the literature the challenge of establishing an optimally interference-avoiding near-field MIMO wireless link, targeting for example modern connected robotics applications in high frequency bands (i.e., mm-wave or terahertz (THz).) We recall that near-field effects, which make conventional directional array-response modeling non-applicable, are extended considerably when the diameter of focused antennas exceeds half the wavelength of the carrier or as the carrier wavelength decreases. As a measure of the interference experienced by an activated MIMO link in the near or far-field, we utilize the conventional SINR metric which is independent of information symbol alphabet specifics. Specifically, we investigate the optimization of the transmitter beam weight vector and the time-domain wave shaping code to maximize the pre-detection SINR at the output of the joint space-time receiver filter for any locally sensed space-time disturbance autocorrelation matrix. We propose two new model-based solutions: (a) A disjoint approach that first optimizes the transmitter beam weight vector and then shapes a digitally coded waveform occupying the entire device accessible frequency band and (b) an optimization approach where the transmitter beam weight vector and the digitally coded waveform are jointly optimized. Our contributions can be summarized as follows:

- We propose two novel closed-loop transmit space-time signal design solutions to dynamically maximize the SINR at the output of the receiver's space-time matched filter for any locally sensed space-time disturbance autocorrelation matrix. The first solution involves searching for an optimized transmitter beam weight vector and separate a posteriori optimization of a digital wave shape code. The second solution involves jointly optimizing the transmitter beam weights and the code vector at increased computational complexity (a mixed integer programming problem.)
- Extensive simulations are carried out to evaluate and compare the effectiveness of the proposed methods under various interference scenarios, including near-field and far-field, spread-spectrum and non-spread-spectrum interference, in light and dense disturbance scenarios. The simulation studies consider varying transmit beam

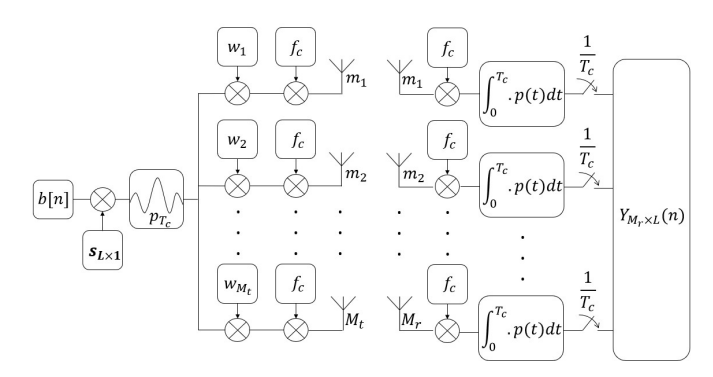


Fig. 1. MIMO system model.

vector and waveform code length and demonstrate the potential of these near/far-field agnostic schemes to dynamically support MIMO links in extreme interference environments.

The rest of the paper is organized as follows. Section II introduces the general MIMO signal model and notation. Section III describes in detail the sensing, data structure formation and optimization problem, whereas Section IV presents the two proposed optimum waveform design options. Section V is devoted to simulation studies and comparisons. Conclusions are drawn in Section VI.

Notation: In this paper, matrices are denoted by upper-case bold letters, column vectors by lower-case bold letters, and scalars by lower-case plain-font letters. The transpose operation is represented by the superscript T , conjugation by * , the Hermitian operation (conjugate transpose) by H , and the Kronecker product by \otimes .

II. MIMO SYSTEM MODEL AND NOTATION

We consider an arbitrary multi-antenna (MIMO) link configuration with M_t transmit and M_r receive antennas as seen in Fig. 1. Without loss of generality, we assume that the transmitter sends an information bit sequence $b(n) \in \{\pm 1\}$, $n = 0, 1, \ldots, N$, at rate $1/T_b$ across all antennas on a carrier frequency f_c using an underlying digitally shaped waveform s(t) of duration T_b . Specifically, the signal transmitted by the m_t th transmit antenna, $m_t = 1, 2, \ldots, M_t$, is represented by

$$x_{m_t}(t) = \sqrt{E_t} \sum_{n=0}^{N-1} b(n)s(t - nT_b)e^{j2\pi f_c t} w_{m_t}$$
 (1)

where E_t is the transmitted energy per bit per antenna, $w_{m_t} \in \mathbb{C}$ is the complex antenna beam weight parameter and the digitally pulse-coded waveform s(t) is given by

$$s(t) = \sum_{l=0}^{L-1} s(l) p_{T_c} (t - lT_c)$$
 (2)

where $\mathbf{s}(l) \in \{\pm 1/\sqrt{L}\}$ is the lth code bit of the code vector $\mathbf{s}_{L\times 1}$, and $p_{T_c}(.)$ is a square-root raised cosine (SRRC) pulse with roll-off factor α and duration T_c where $T_b = LT_c$ and the bandwidth of the transmitted signal is $\beta = (1+\alpha)/T_c$. For clarity in presentation, it is assumed that the individual

pulses are normalized to unit energy

$$\int_{0}^{T_c} |p_{Tc}(t)|^2 dt = 1.$$
 (3)

The receiver consists of M_r antenna elements. After carrier demodulation of the transmitted signal, the receiving antennas capture

$$\mathbf{r}_{M_r \times 1}(t) = \sqrt{E_t} \sum_{n=0}^{N-1} b(n)s(t - nT_b)\mathbf{H}^T \mathbf{w}_{M_t} + \mathbf{i}(t) + \mathbf{n}(t)$$

where $\mathbf{H} \in \mathbb{C}^{M_t \times M_r}$ is a generic channel matrix assumed to remain constant over NT_b sec,

$$\mathbf{H} \triangleq \begin{bmatrix} h_{1,1} & h_{1,2} & \dots & h_{1,M_r} \\ h_{2,1} & h_{2,2} & \dots & h_{2,M_r} \\ \vdots & \vdots & \ddots & \vdots \\ h_{M_t,1} & h_{M_t,2} & \dots & h_{M_t,M_r} \end{bmatrix}$$
(5)

where $h_{m_t,m_r} \in \mathbb{C}$ is the complex coefficient of the channel between the m_t th transmit antenna and the m_r th receive antenna. We recall that if two transmit antennas $m_t = i, j$ are in the far-field of a receive antenna $m_r = k$, then $h_{i,k}$ and $h_{j,k}$ have approximately equal phase (and amplitude), which enables effective directional signal reception by an appropriately set receiver array. Instead, if the two transmit antennas $m_t = i, j$ are in the near-field of $m_r = k$, then the phase of $h_{i,k}$ and $h_{j,k}$ vary significantly. Conventionally, we set the beginnings of the far field at the distance at which the experienced phase difference is less than $\pi/8$ (Fraunhofer distance) [32]. Returning to the description of (4), $\mathbf{w}_{M_t} \in \mathbb{C}^{M_t}$ is the transmitter beam weight vector, $\mathbf{n}(t) \in \mathbb{C}^{M_r \times 1}$ denotes a complex Gaussian noise process that is assumed white both in time and space, and $\mathbf{i}(t) \in \mathbb{C}^{M_r}$ models comprehensively environmental disturbance of any other form.

For a given fixed bit period $n, n = 1, 2, \ldots, N$, upon pulse matched-filtering and sampling over L pulses at each receive antenna element, the collected values are organized in the form of a space-time data matrix $\mathbf{Y}_{M_r \times L}(n)$ (see Fig. 1). The data matrix is then vectorized to

$$\mathbf{y}_{M_rL\times 1}(n) = Vec\{\mathbf{Y}_{M_r\times L}(n)\} =$$

$$= \sqrt{E_t}b(n)(\mathbf{s}\otimes \mathbf{H}^T)\mathbf{w}_{M_t} + \mathbf{i}(n) + \mathbf{n}(n) \quad (6)$$

where $\mathbf{i}(n)$ and $\mathbf{n}(n)$ represent post pulse-matched-filtering interference and white noise in the space-time receiver domain. In the following section, we derive the maximum-SINR optimal joint space-time receiver filter in the M_rL product vector space and we find its output SINR as a function of s (time-domain code) and \mathbf{w}_{M_t} (transmit beam vector), creating therefore the foundation for space and time transmit waveform optimization (closed-loop interference avoiding space and time precoding.)

III. SENSING AND THE WAVEFORM OPTIMIZATION PROBLEM

For the given received space-time data vector in (6), the space-time receiver matched filter (MF) is by definition

given by

$$\mathbf{w}_{\mathrm{MF}} \triangleq E\left\{\mathbf{y}_{M_rL \times 1}(n) \ b(n)\right\} = (\mathbf{s} \otimes \mathbf{H}^T)\mathbf{w}_{M_t}. \tag{7}$$

The compound space-time disturbance $\mathbf{i}(n) + \mathbf{n}(n)$, assumed to be zero mean for simplicity, has autocorrelation/autocovariance matrix defined by

$$\mathbf{R}_{i+n} \triangleq E\left\{ \left(\mathbf{i}(n) + \mathbf{n}(n)\right) \left(\mathbf{i}(n) + \mathbf{n}(n)\right)^{H} \right\} \in \mathbb{C}^{M_r L \times M_r L}.$$
(8)

In view of (7) and (8), the space-time maximum SINR receiver filter becomes

$$\mathbf{w}_{\text{max-SINR}} = k \, \mathbf{R}_{i+n}^{-1} (\mathbf{s} \otimes \mathbf{H}^T) \mathbf{w}_{M_t}, \, k \in \mathbb{C}.$$
 (9)

We can now calculate the output SINR of the maximum SINR space-time receiver filter as follows,

$$\operatorname{SINR}(\mathbf{s}, \mathbf{w}_{M_t}) \\
\triangleq \frac{\operatorname{E}\left\{\left|\mathbf{w}_{\max-\operatorname{SINR}}^{H}\left(\sqrt{E_t}b(n)(\mathbf{s} \otimes \mathbf{H}^{T})\mathbf{w}_{M_t}\right)\right|^{2}\right\}}{\operatorname{E}\left\{\left|\mathbf{w}_{\max-\operatorname{SINR}}^{H}\left(\mathbf{i}(n) + \mathbf{n}(n)\right)\right|^{2}\right\}} \\
= E_t\left[\left(\mathbf{s} \otimes \mathbf{H}^{T}\right)\mathbf{w}_{M_t}\right]^{H} \mathbf{R}_{i+n}^{-1}(\mathbf{s} \otimes \mathbf{H}^{T})\mathbf{w}_{M_t}. \tag{10}$$

We see, therefore, that the SINR at the output of the maximum SINR space-time receiver filter for the general near-field MIMO link model under examination is a closed form expression of the transmit beam weight vector $\mathbf{w}_{M_t} \in \mathbb{C}^{M_t}$ and the time domain code vector $\mathbf{s} \in \{\pm 1/\sqrt{L}\}^L$. It is of interest, then, to investigate what waveform design values \mathbf{w}_{M_t} and \mathbf{s} maximize the maximum attainable SINR by the receiver filter for a locally sensed space-time disturbance-only autocorrelation matrix

$$\widehat{\mathbf{R}}_{i+n} = \sum_{k=1}^{K} (\mathbf{i}(k) + \mathbf{n}(k)) (\mathbf{i}(k) + \mathbf{n}(k))^{H}$$
(11)

over K samples and estimated MIMO channel state information matrix \mathbf{H} .

In the following section, we present two distinct space-time waveform design methods.

IV. SPACE-TIME WAVEFORM DESIGN

In this section, we develop and describe in implementation detail two space-time waveform design methods. The first method carries out disjoint space-first, time-next optimization, i.e., we first suggest an optimized transmit beam weight vector \mathbf{w}_{M_t} and then find the conditionally optimal code vector \mathbf{s} given \mathbf{w}_{M_t} . The second method that we present produces a jointly optimal $(\mathbf{w}_{M_t}, \mathbf{s})$ pair.

A. Disjoint Space and Time Optimization

We concentrate first in the space domain operation. Considering only the lth column of the data matrix $\mathbf{Y}_{M_r \times L}(n)$ in Fig. 1 and following the notation in (4), we have

$$\mathbf{y}_{l}(n) = \sqrt{E_{t}}b(n)s(l)\mathbf{H}^{T}\mathbf{w}_{M_{t}} + \mathbf{i}(l,n) + \mathbf{n}(l,n) \in \mathbb{C}^{M_{r}},$$
(12)

Algorithm 1: Disjoint space and time optimization

Input: Pulse-filtered interference-plus-noise received samples; estimated channel matrix $\mathbf{H} \in \mathbb{C}^{M_t \times M_r}$.

- Calculate (estimate) space-only disturbance autocorrelation matrix $\mathbf{R_{i+n}^s} \in \mathbb{C}^{M_r \times M_r}$ in (13).
- Calculate minimum-eigenvalue eigenvector of \mathbf{R}_{i+n}^s , $\mathbf{q}_{space} \in \mathbb{C}^{M_r}$.
- If $M_t = M_r$, $\mathbf{w}_{M_t}^{opt} = inv(\mathbf{H}^T)\mathbf{q}_{space}$. If $M_t \neq M_r$, $\mathbf{w}_{M_t}^{opt} = inv(\mathbf{H}\mathbf{H}^T)\mathbf{H}\mathbf{q}_{space}$.
- Find optimum code $\mathbf{s}^{opt} \in \{\pm 1/\sqrt{L}\}^{L}$ (or other alphabet) by discrete search over (19).

Output: $\mathbf{w}_{M_t}^{opt}$, \mathbf{s}^{opt} .

Fig. 2. Proposed disjoint first-space, then-time optimization algorithm.

 $l \in \{1, 2, \dots, L\}, n \in \{1, 2, \dots, N\}.$ The space-only disturbance autocorrelation matrix is defined by

$$\mathbf{R}_{i+n}^{s} \triangleq E\left\{ \left(\mathbf{i}(l,n) + \mathbf{n}(l,n) \right) \left(\mathbf{i}(l,n) + \mathbf{n}(l,n) \right)^{H} \right\} \in \mathbb{C}^{M_r \times M_r};$$
(13)

the space-only maximum SINR filter is

$$\mathbf{w}_{\text{max-SINR}} = k \mathbf{R}_{i+n}^{s^{-1}} \mathbf{H}^T \mathbf{w}_{M_t} \in \mathbb{C}^{M_r}, k \in \mathbb{C};$$
 (14)

and its output SINR is

$$SINR(\mathbf{w}_{M_t}) = E_t \left(\mathbf{H}^T \mathbf{w}_{M_t} \right)^H \mathbf{R}_{i+n}^{s^{-1}} \left(\mathbf{H}^T \mathbf{w}_{M_t} \right). \tag{15}$$

By (15) (a quadratic expression in $\mathbf{H}^T \mathbf{w}_{M_t}$), we recognize that if $\mathbf{q}_{space} \in \mathbb{C}^{M_r}$ is the maximum-eigenvalue eigenvector of the space domain inverse disturbance autocorrelation matrix \mathbf{R}_{i+n}^{s-1} , then the maximum SINR optimal beam weight vector $\mathbf{w}_{M_t}^{opt}$ is such that

$$\mathbf{H}^T \mathbf{w}_{M_t}^{opt} = \mathbf{q}_{space}. \tag{16}$$

If $M_t = M_r$ and $\mathbf{H} \in \mathbb{C}^{(M_t = M_r) \times (M_t = M_r)}$ is full rank, then

$$\mathbf{w}_{M_{\star}}^{opt} = inv(\mathbf{H}^T)\mathbf{q}_{space}.$$
 (17)

If $M_t \neq M_r$ and $\mathbf{H}\mathbf{H}^T$ is full rank (i.e., $M_t < M_r$), then we calculate

$$\mathbf{w}_{M_t}^{opt} = inv(\mathbf{H}\mathbf{H}^T)\mathbf{H}\mathbf{q}_{space}.$$
 (18)

The next step is to search for a binary antipodal code sequence $\mathbf{s} \in \{\pm 1/\sqrt{L}\}^L$ so that the corresponding final space-time post-filtering SINR(s, $\mathbf{w}_{M_t}^{opt}$) is maximized. Utilizing (10) for fixed $\mathbf{w}_{M_t} = \mathbf{w}_{M_t}^{opt}$, the remaining optimization problem can be written as

$$\mathbf{s}^{\text{opt}} = \underset{\mathbf{s} \in \{\pm 1/\sqrt{L}\}^{L}}{\operatorname{argmax}} \left\{ \left[(\mathbf{s} \otimes \mathbf{H}^{T}) \mathbf{w}_{M_{t}}^{opt} \right]^{H} \mathbf{R}_{i+n}^{-1} (\mathbf{s} \otimes \mathbf{H}^{T}) \mathbf{w}_{M_{t}}^{opt} \right\}$$
(19)

where $\mathbf{R}_{i+n} \in \mathbb{C}^{M_rL \times M_rL}$ is the joint space-time disturbance autocorreation matrix defined by (8). An optimized code sequence for the given $\mathbf{w}_{M_t}^{opt}$ transmit beam vector can be

Algorithm 2: Joint space-time optimization

Input: Pulse-filtered interference-plus-noise received samples; estimated channel matrix $\mathbf{H} \in \mathbb{C}^{M_t \times M_r}$.

- Calculate (estimate) space-time disturbance autocorrelation matrix $\mathbf{R}_{i+n} \in \mathbb{C}^{M_rL \times M_rL}$ in (21).
- Calculate minimum-eigenvalue eigenvector of \mathbf{R}_{i+n} , $\mathbf{q}_{s-t} \in \mathbb{C}^{M_rL}$.
- Find optimum code $\mathbf{s}^{opt} \in \{\pm 1/\sqrt{L}\}^L$ (or other alphabet) by discrete search over (24).
- Find jointly optimal beam weight vector $\mathbf{w}_{M_t}^{opt}$ by inserting s^{opt} in (23).

Output: $\mathbf{w}_{M_t}^{opt}$, \mathbf{s}^{opt} .

Fig. 3. Proposed joint space-time optimization algorithm.

found by an one-dimensional search over 2^L candidate code sequences. The complete disjoint space and time optimization algorithm is summarized in Fig. 2 for easy reference. Its overall computational complexity is $\mathcal{O}(2M_t^3 + (M_rL)^3 +$ $4M_tM_rL + 4M_tM_r + 2^{L-1}$) (the code-vector quadratic optimization sub-problem is sign insensitive.)

The separately optimized code and transmit beam weight vectors \mathbf{s}^{opt} , $\mathbf{w}_{M_t}^{opt}$ define the interference-avoiding MIMO link waveform. Under the assumption that $\mathbf{s}^{opt}, \mathbf{w}_{M_t}^{opt}$ are made available to the transmitter within the **H** and \mathbf{R}_{i+n} channel coherence time, the output SINR of the joint space-time receiver filter is conditionally maximized at operational information rate $1/LT_c$ symbols per second where T_c is the duration of the utilized SRRC pulse.

B. Joint Space-Time Optimization

We now revisit (10) and attempt to jointly optimize s and \mathbf{w}_{M_t} ; that is, we attempt to solve

$$(\mathbf{s}^{opt}, \mathbf{w}_{M_t}^{opt}) = \underset{\mathbf{s} \in \{\pm 1/\sqrt{L}\}^L, \mathbf{w}_{M_t} \in \mathbb{C}^{M_t}}{\operatorname{argmax}} \times \left\{ \left[(\mathbf{s} \otimes \mathbf{H}^T) \mathbf{w}_{M_t} \right]^H \mathbf{R}_{i+n}^{-1} (\mathbf{s} \otimes \mathbf{H}^T) \mathbf{w}_{M_t} \right\}.$$
(20)

From (20), we recognize that -code domain and MIMO channel specifics aside- the overall jointly optimal space-time waveform is the maximum-eigenvalue eigenvector $\mathbf{q}_{s-t} \in$ \mathbb{C}^{M_rL} of the inverse of the joint space-time disturbance autocorrelation matrix

$$\mathbf{R}_{i+n} \triangleq E\left\{ \left(\mathbf{i}(n) + \mathbf{n}(n)\right) \left(\mathbf{i}(n) + \mathbf{n}(n)\right)^{H} \right\} \in \mathbb{C}^{M_r L \times M_r L},$$
(21)

which coincides with the smallest-eigenvalue eigenvector of \mathbf{R}_{i+n} . As an effective surrogate to the mixed-integer optimization problem in (20), we suggest l_2 -norm approximation of \mathbf{q}_{s-t} by $(\mathbf{s} \otimes \mathbf{H}^T)\mathbf{w}_{M_t}$, i.e., we try to solve

$$(\mathbf{s}^{opt}, \mathbf{w}_{M_t}^{opt}) = \underset{\mathbf{s} \in \{\pm 1/\sqrt{L}\}^L, \mathbf{w}_{M_t} \in \mathbb{C}^{M_t}}{\operatorname{argmin}} ||\mathbf{q}_{s-t} - (\mathbf{s} \otimes \mathbf{H}^T) \mathbf{w}_{M_t}||^2. \quad (22)$$

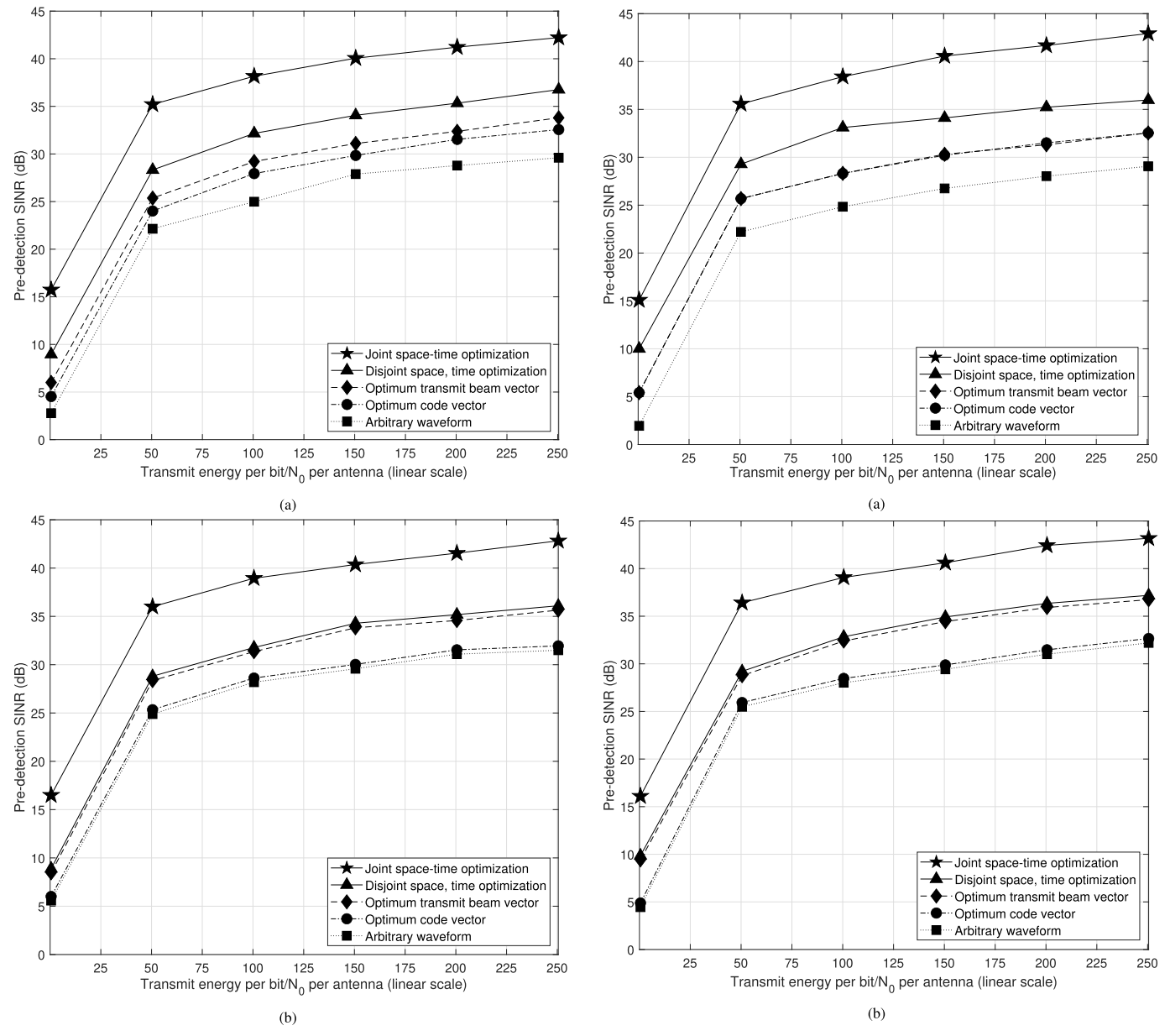


Fig. 4. Pre-detection SINR in light near-field non-spread-spectrum interference ($M_t=M_r=M_{i_1}=4$): (a) L = 4, (b) L = 16.

Fig. 5. Pre-detection SINR in dense near-field non-spread-spectrum interference ($M_t=M_r=M_{i_1}=4$): (a) L = 4, (b) L = 16.

We can prove (see Appendix) that a closed-form expression of $\mathbf{w}_{M\star}^{opt}$ for any fixed code vector \mathbf{s} is

$$\mathbf{w}_{M_{\bullet}}^{opt} = inv[(\mathbf{s}^T \otimes \mathbf{H}^*)(\mathbf{s} \otimes \mathbf{H}^T)](\mathbf{s}^T \otimes \mathbf{H}^*)\mathbf{q}_{s-t}$$
 (23)

where $(\mathbf{s}^T \otimes \mathbf{H}^*)(\mathbf{s} \otimes \mathbf{H}^T)$ is invertible if $rank(\mathbf{H}) \geq M_t$. Inserting now (23) in (22) (or (20)), we can find the jointly optimal code vector \mathbf{s}^{opt} with a simple binary search

$$\mathbf{s}^{opt}$$

$$= \underset{\mathbf{s} \in \{\pm 1/\sqrt{L}\}^{L}}{\operatorname{argmin}} ||\mathbf{q}_{s-t}|$$

$$- (\mathbf{s} \otimes \mathbf{H}^{T}) inv[(\mathbf{s}^{T} \otimes \mathbf{H}^{*})(\mathbf{s} \otimes \mathbf{H}^{T})](\mathbf{s}^{T} \otimes \mathbf{H}^{*})\mathbf{q}_{s-t}||^{2}$$

$$= \underset{\mathbf{s} \in \{\pm 1/\sqrt{L}\}^{L}}{\operatorname{argmin}} ||\{\mathbf{I} \\ - (\mathbf{s} \otimes \mathbf{H}^{T})[(\mathbf{s}^{T} \otimes \mathbf{H}^{*})(\mathbf{s} \otimes \mathbf{H}^{T})]^{-1}(\mathbf{s}^{T} \otimes \mathbf{H}^{*})\}\mathbf{q}_{s-t}||^{2}$$

$$(24)$$

where **I** is the $M_rL \times M_rL$ identity matrix. Reverting to (23), we calculate $\mathbf{w}_{M_t}^{opt}$. The overall joint space-time optimization algorithm is summarized for easy reference in Fig. 3. The computational complexity is $\mathcal{O}(M_t^3 + M_t^2 + M_t^2 M_r L + 4M_t M_r L + 2^{L-1})$.

It is of interest to mention that to the extend that our joint design of \mathbf{s}^{opt} and $\mathbf{w}_{M_t}^{opt}$ by (22) succeeds in approximating closely the eigenvector \mathbf{q}_{s-t} , i.e., $(\mathbf{s}^{opt} \otimes \mathbf{H}^T)\mathbf{w}_{M_t}^{opt} \approx \mathbf{q}_{s-t}$, then $\mathbf{R}_{i+n}^{-1}(\mathbf{s}^{opt} \otimes \mathbf{H}^T)\mathbf{w}_{M_t}^{opt} = c(\mathbf{s}^{opt} \otimes \mathbf{H}^T)\mathbf{w}_{M_t}^{opt}$, $c \in \mathbb{C}$. Therefore, the space-time maximum SINR receiver filter $\mathbf{w}_{\max-\text{SINR}} = k \mathbf{R}_{i+n}^{-1}(\mathbf{s} \otimes \mathbf{H}^T)\mathbf{w}_{M_t}$, $k \in \mathbb{C}$, degenerates conveniently to the matched-filter (MF) $(\mathbf{s}^{opt} \otimes \mathbf{H}^T)\mathbf{w}_{M_t}^{opt}$. As before, the operational information rate of the link is $1/LT_c$ symbols per second where T_c is the duration of the utilized SRRC pulse.

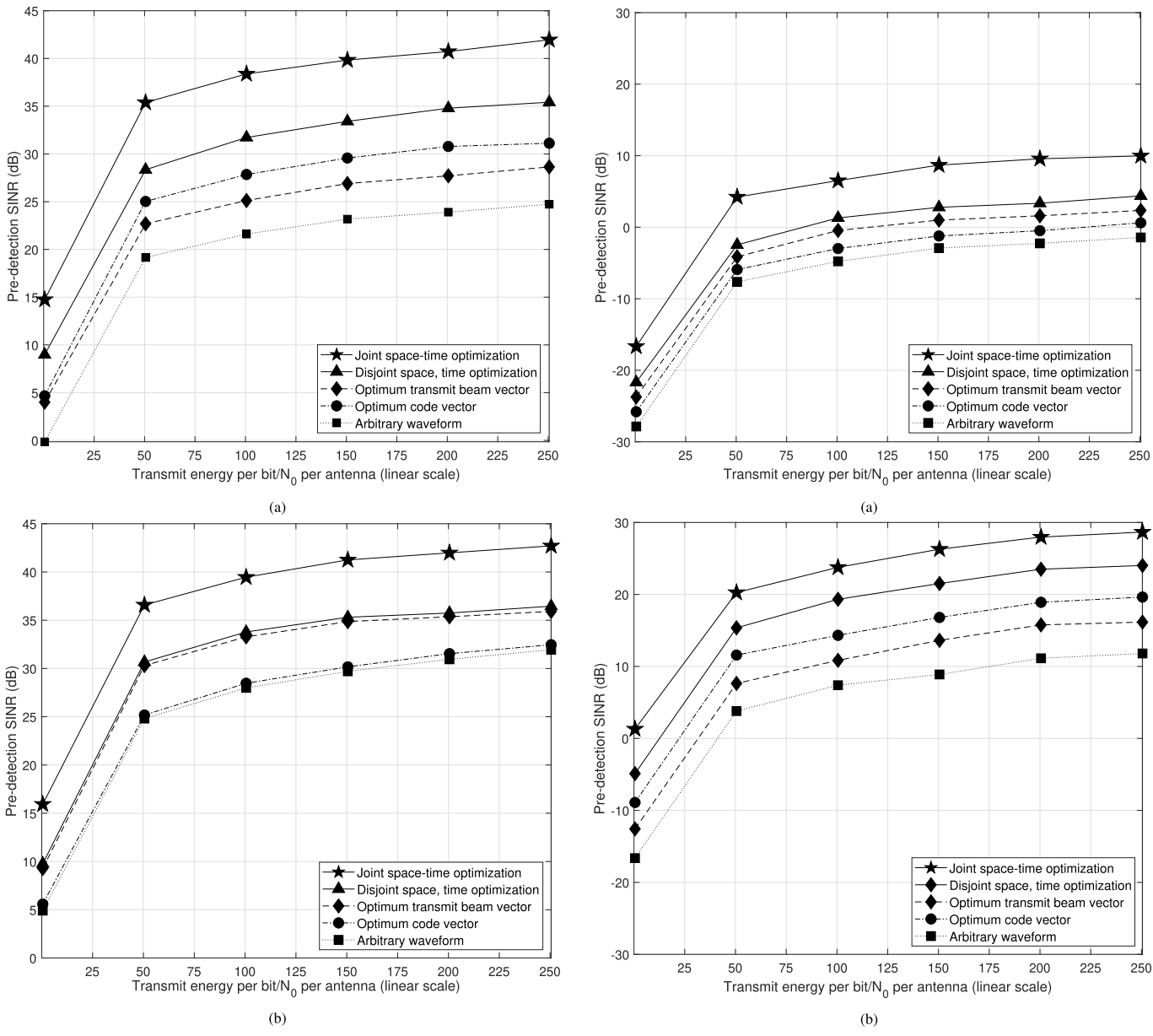


Fig. 6. Pre-detection SINR in light near-field spread-spectrum interference ($M_t=M_r=M_{i_2}=4$): (a) L = 4, (b) L = 16.

Fig. 7. Pre-detection SINR in dense near-field spread-spectrum interference ($M_t=M_r=M_{i_2}=4$): (a) L = 4, (b) L = 16.

V. SIMULATIONS STUDIES AND COMPARISONS

This section presents simulation results that demonstrate the effectiveness of the proposed formal MIMO waveform optimization methods using as direct performance evaluation metric the SINR at the output of the maximum-SINR spacetime receiver filter. To model disturbance effects, we consider near-field/far-field and spread-spectrum/non-spread-spectrum interference signals in all four possible combinations. We evaluate the performance of the proposed waveforms in light and dense interference, where in the light interference scenario we assume there are $M_r/2$ interfering transmitters of each interference type and in the dense interference scenario $5M_r$ interfering transmitters of each interference type. In all studies, the data record size used to estimate the disturbance autocorrelation matrix needed for the computation of $\mathbf{w}_{M_t}^{opt}$ and \mathbf{s}^{opt} by Fig. 2 or Fig. 3 and the computation of $\mathbf{w}_{\max-\text{SINR}}^{opt}$ by (9) is set to N=100.

All presented results are averages over 10000 independent experiments.

In particular, near-field non-spread-spectrum interfering signals are described by

$$\mathbf{i}_1(t) = \sqrt{E_1} \sum_n b_1[n] p(t - nT_b) \mathbf{H}_1^T \mathbf{w}_{M_{t_1}},$$
 (25)

with bandwidth $\frac{1}{T_b}$, $\mathbf{w}_{M_{t_1}}$ transmit antennas, $b_1[n] \in \{\pm 1\}$, and $\mathbf{H}_1 \in \mathbb{C}^{M_{t_1} \times M_r}$. Near-field spread-spectrum interfering signals are described by

$$\mathbf{i}_2(t) = \sqrt{E_2} \sum_n b_2[n] s_2(t - nT_b) \mathbf{H}_2^T \mathbf{w}_{M_{t_2}},$$
 (26)

$$\mathbf{s}_{2}(t) = \sum_{l=0}^{L-1} \mathbf{s}_{2}(l) p_{T_{c}}(t - lT_{c}), \qquad (27)$$

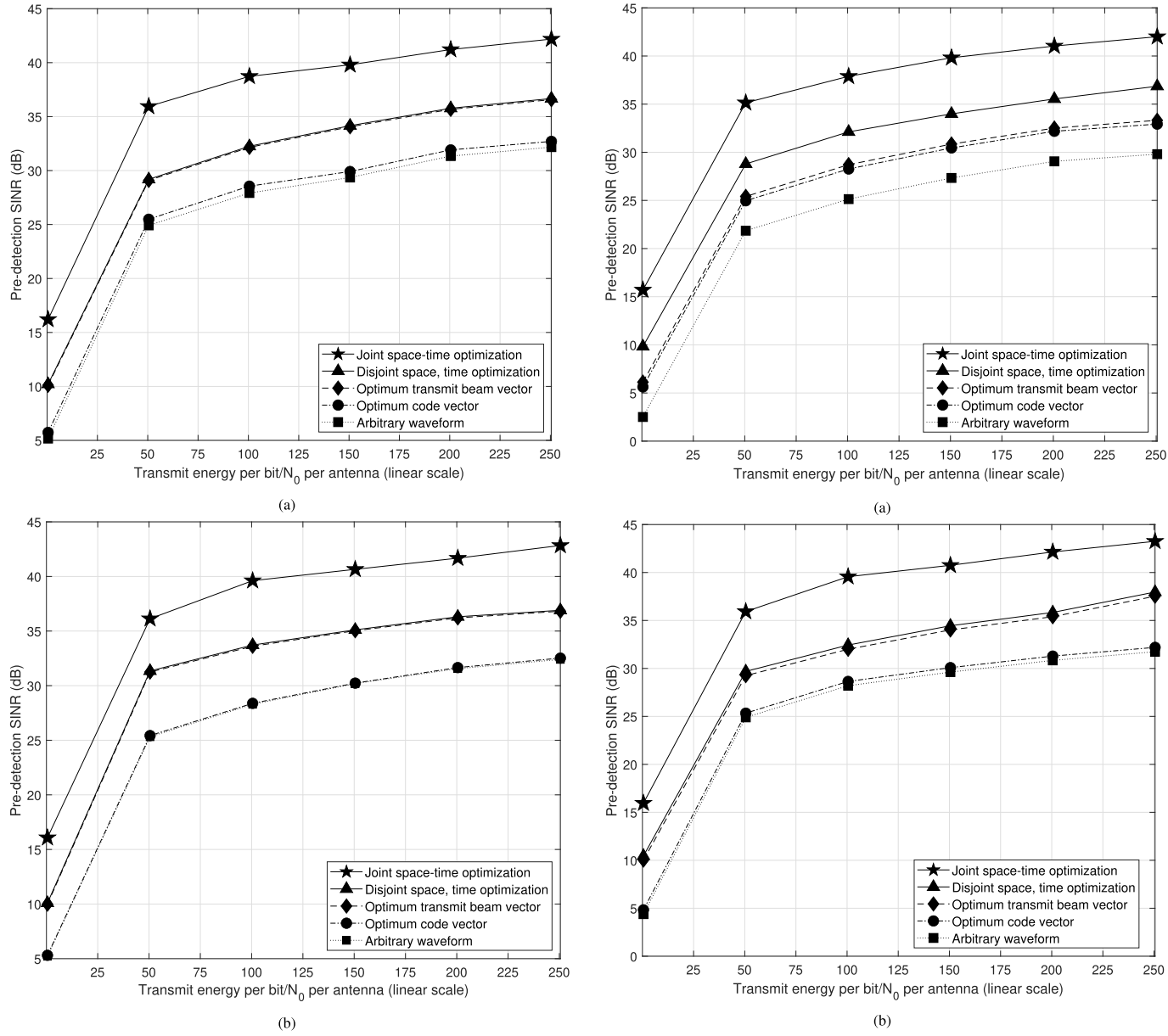


Fig. 8. Pre-detection SINR in light far-field non-spread-spectrum interference ($M_t=M_r=M_{i_3}=4$): (a) L = 4, (b) L = 16.

Fig. 9. Pre-detection SINR in dense far-field non-spread-spectrum interference ($M_t = M_r = M_{i_3} = 4$): (a) L = 4, (b) L = 16.

with bandwidth $\frac{L}{T_b}$, $\mathbf{s}_2(l) \in \{\pm 1/\sqrt{L}\}$, $\mathbf{w}_{M_{t_2}}$ transmit antennas, $b_2[n] \in \{\pm 1\}$, and $\mathbf{H}_2 \in \mathbb{C}^{M_{t_2} \times M_r}$.

Far-field interfering signals have a directional interference effect on the M_r -element receiver front, which is modeled herein by an array response vector that assumes for simplicity linear uniform geometry and inter-element spacing equal to half the carrier wavelength. In particular, far-field non-spread-spectrum interfering signals are described by

$$\mathbf{i}_3(t) = \sqrt{E_3} \sum_n b_3[n] p(t - nT_b) h_3 \mathbf{a}(\theta_3),$$
 (28)

with bandwidth $\frac{1}{T_b}$, $b_3[n] \in \{\pm 1\}$, flat-fading coefficient $h_3 \in \mathbb{C}$, and array response vector $\mathbf{a}(\theta_3) \in \mathbb{C}^{M_r}$ with angle of arrival $\theta_3 \in (-\frac{\pi}{2}, \frac{\pi}{2})$. Far-field spread-spectrum interfering

signals are described by

$$\mathbf{i}_4(t) = \sqrt{E_4} \sum_n b_4[n] s_4(t - nT_b) h_4 \mathbf{a}(\theta_4),$$
 (29)

$$\mathbf{s}_4(t) = \sum_{l=0}^{L-1} \mathbf{s}_4(l) p_{T_c} (t - lT_c), \qquad (30)$$

with bandwidth $\frac{L}{T_b}$, $\mathbf{s}_4(l) \in \{\pm 1/\sqrt{L}\}$, flat-fading coefficient $h_4 \in \mathbb{C}$, and array response vector $\mathbf{a}(\theta_4) \in \mathbb{C}^{M_r}$ with angle of arrival $\theta_4 \in (-\frac{\pi}{2}, \frac{\pi}{2})$.

In Fig. 4, we study the pre-detection SINR of a MIMO link with $M_t=M_r=4$ antennas in light near-field non-spread-spectrum interference under no waveform optimization, code only optimization, transmit beam vector only optimization, disjoint transmit beam vector optimization followed by code vector optimization, and joint beam-code optimization. The number of transmit antennas of each of the $M_r/2=2$

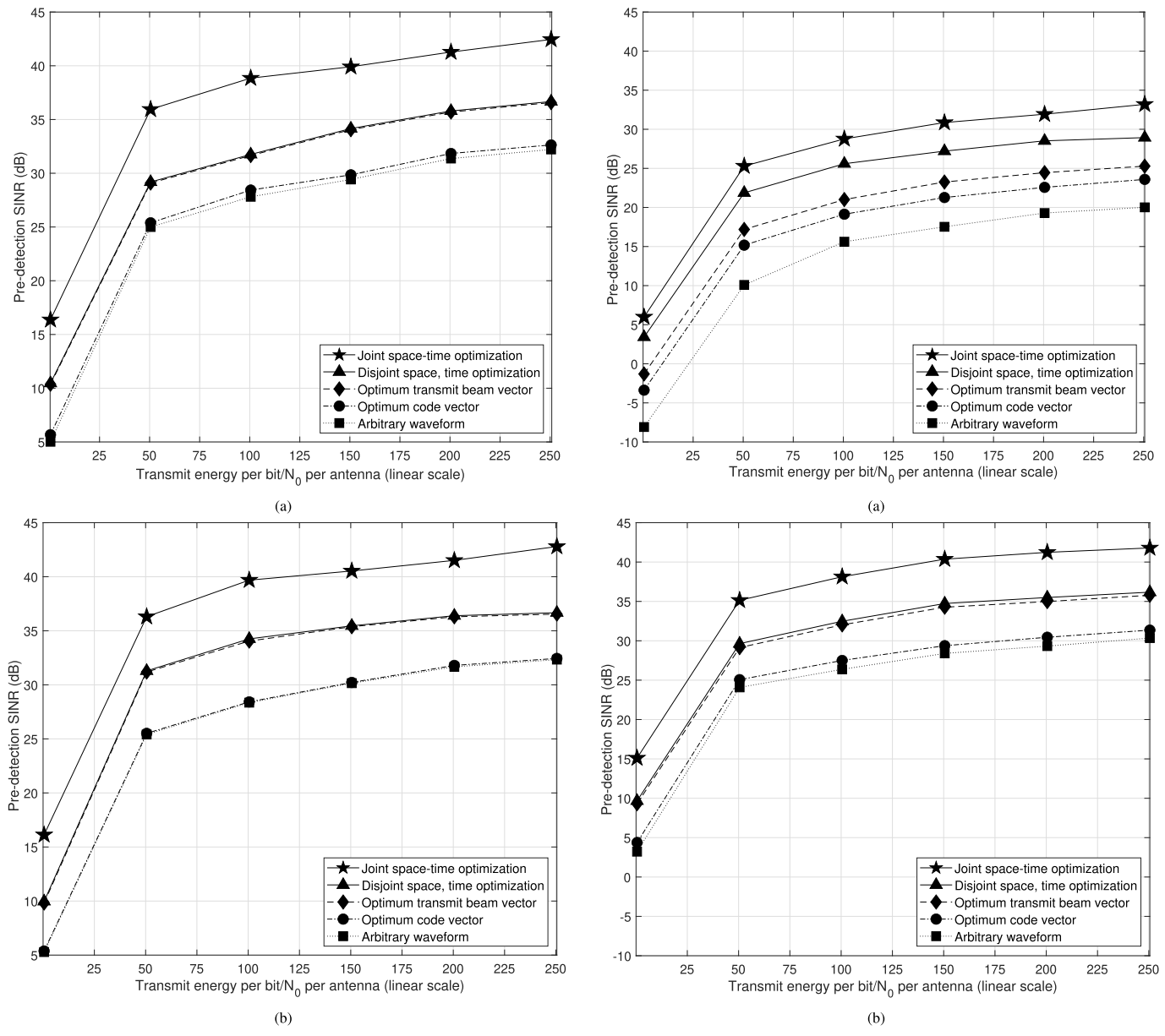


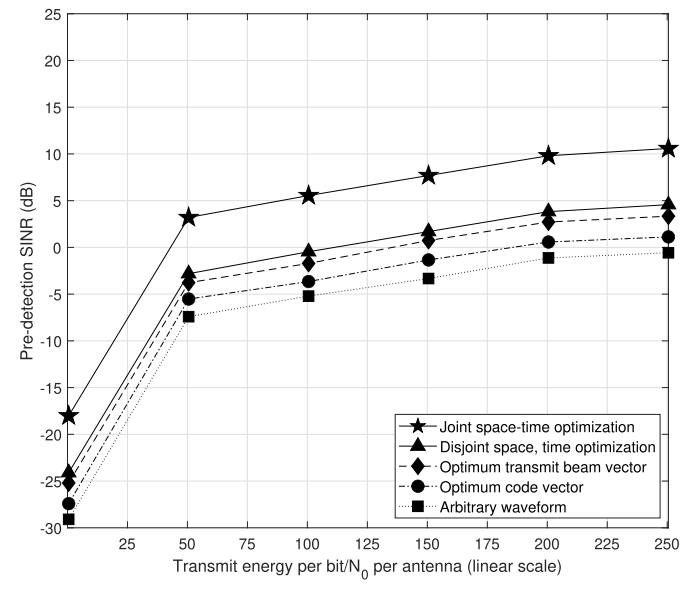
Fig. 10. Pre-detection SINR in light far-field spread-spectrum interference $(M_t=M_r=M_{i_4}=4)$: (a) L = 4, (b) L = 16.

Fig. 11. Pre-detection SINR in dense far-field spread-spectrum interference $(M_t = M_r = M_{i_4} = 4)$: (a) L = 4, (b) L = 16.

interferers is $M_{i_1} = 4$ and their energy-per-bit-over- N_0 value per antenna is set at 10dB where $N_0/2$ denotes the power spectral density of the underlying Gaussian vector noise process assumed to be white across time and space (antenna points). Fig. 4(a) assumes codelength L=4 and Fig. 4(b) assumes codelength L = 16. Figs. 5(a) and 5(b) repeat the same studies for dense near-field non-spread-spectrum interference (i.e., $5M_r = 20$ interferers) with energy-perbit-over- N_0 value per antenna equal to 15dB. An overall observation is that the MIMO link easily handles light or dense near-field non-spread-spectrum interference and the joint space-time waveform optimization approach offer 6dB or more gain over the disjoint space first, time next optimization approach at any transmit-energy-per-bit per antenna level. For example, a target pre-detection SINR value equal to 15dB(practically error-free binary phase-shift-keying decoding) is attained by joint space-time optimization at about 1/15th of the transmit-energy-per-bit per antenna required under disjoint optimization. Comparing against no optimization whatsoever (arbitrary waveform), the fraction becomes 1/35. Finally, as expected, for large codelengths, beam vector optimization only and beam vector optimization followed by code vector optimization have about the same pre-detection SINR yield (Figs. 4(b) and 5(b).)

Figs. 6 and 7 repeat the studies of Figs. 4 and 5 under the more challenging scenario of spread-spectrum near-field interference with codelengths that follow the codelength of the main link. The trends and gains in favor of joint space-time optimization remain the same, but Fig. 7(a) highlights the difficulty in dealing with dense near-field spread-spectrum disturbance and the importance of having sufficiently large codelength to operate and optimize (Fig. 7(b).)

Figs. 8 and 9 study far-field non-spread-spectrum interference with conclusions similar to the near-field corresponding



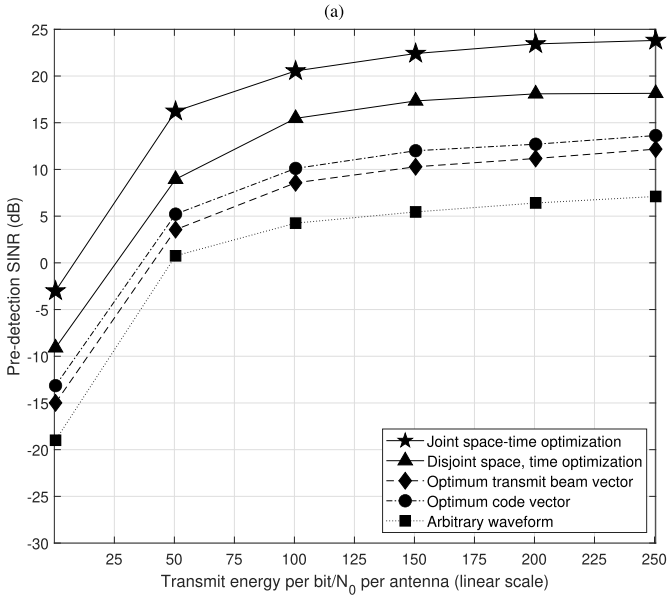


Fig. 12. Pre-detection SINR in dense interference of all types ($M_t=M_r=M_{i_1}=M_{i_2}=M_{i_3}=M_{i_4}=4$): (a) L = 4, (b) L = 16.

case (impressive pre-detection SINR gain by the jointly optimized waveform.)

Figs. 10 and 11 study spread-spectrum far-field interference, regarded arguably as a simpler case than its near-field counterpart. Indeed, optimized waveforms handle well dense far-field spread-spectrum interference even with small codelengths (see for example Fig. 11(a).)

Fig. 12 adds up all types of interference in their dense form, that is, twenty near-field and twenty far-field non-spread-spectrum interferers, as well as twenty near-field and twenty far-field spread-spectrum interferers, all at 15dB energy-per-bit-over- N_0 value per transmit antenna. Given sufficient degrees of freedom in the time domain, such as L=16 in Fig. 12(b), the two proposed disjointly and jointly optimized MIMO waveforms readily attain 10dB and 15dB pre-detection SINR, correspondingly.

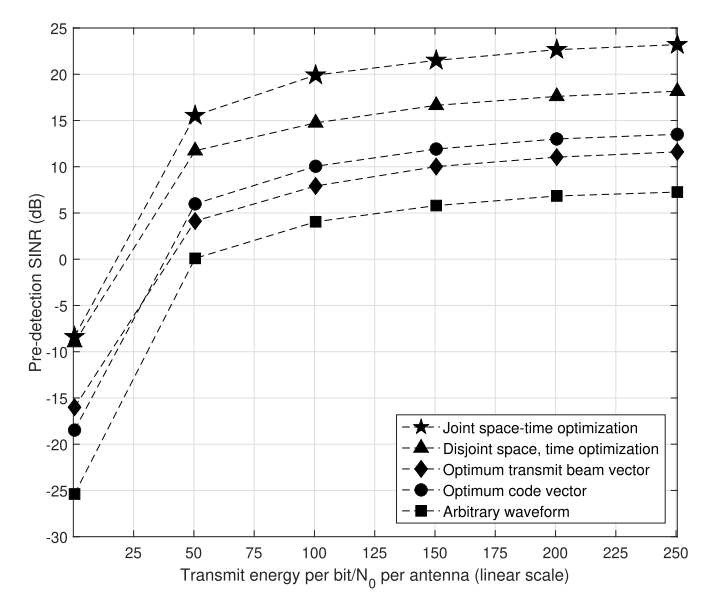


Fig. 13. Pre-detection SINR under imperfect channel knowledge in dense interference of all types ($M_t=M_r=M_{i_1}=M_{i_2}=M_{i_3}=M_{i_4}=4$): L. = 16.

All studies presented above assumed perfect channel state information, i.e. knowledge of the MIMO channel matrix $\mathbf{H} \in \mathbb{C}^{M_t \times M_r}$ (as well as perfect pulse/symbol synchronization.) Instead, Fig. 13 reproduces the studies of Fig. 12(b) under imperfect channel knowledge with independent zero-mean complex Gaussian error per channel coefficient and mean-square estimation error $\sigma^2 = \epsilon \times 10^{-E_t/N_0(dB)/10}$ where $\epsilon = 5$ is set to represent the level of channel knowledge imperfection in our study [6] and [7]. A moderate SINR loss is observed compared to Fig. 12(b) that diminishes as the mean-square error decreases for increasing E_t/N_0 values.

VI. CONCLUSION

In this paper, we addressed the challenge of creating a dynamic near-field or far-field MIMO wireless link over a fixed frequency band that may be heavily utilized with application focus autonomous interference-avoiding machine-to-machine communications. In particular, given a running local estimate of the disturbance autocorrelation matrix and the MIMO channel matrix coefficients, we found the optimal transmit beam weight vector and time-domain pulse code that maximize the output SINR of the maximum-SINR joint space-time receiver filter. We proposed and described in implementation detail two algorithmic solutions. The first solution carries out disjoint space-first (transmit beam weight vector) time-next (pulse code sequence) waveform optimization. The second solution succeeds in carrying out jointly optimal transmit beam weight vector and pulse code sequence optimization leaning on the closed-form expression of the optimal transmit beam vector that we derived as a function of the pulse code sequence. Notably, under joint beam weight and code vector optimization the maximum SINR space-time receiver filter simplifies to space-time matched-filtering reception.

Through extensive simulations studies, we evaluated the effectiveness of the methods in the presence of near-field/far-field, spread-spectrum/non-spread spectrum interference,

in both light and dense interference scenarios. The studies highlighted the ability of the optimized waveforms, particularly joint space-time optimization, to maintain "clean" communications in extreme mixed-interference environments (i.e, attained pre-detection SINR of 15dB or better.)

APPENDIX PROOF OF EQUATION (23)

We consider the gradient of the objective function in (22) with respect to $\mathbf{w}_{M_t}^H$. We expand the l_2 -norm and apply the hermitian operator to all components inside the first parenthesis,

$$\nabla_{\mathbf{w}_{M_{t}}^{H}} ||\mathbf{q}_{s-t} - (\mathbf{s} \otimes \mathbf{H}^{T}) \mathbf{w}_{M_{t}}||^{2}$$

$$= \nabla_{\mathbf{w}_{M_{t}}^{H}} [(\mathbf{q}_{s-t} - (\mathbf{s} \otimes \mathbf{H}^{T}) \mathbf{w}_{M_{t}})^{H} (\mathbf{q}_{s-t} - (\mathbf{s} \otimes \mathbf{H}^{T}) \mathbf{w}_{M_{t}})]$$
(31)

$$= \nabla_{\mathbf{w}_{M_t}^H} [(\mathbf{q}_{s-t}^H - \mathbf{w}_{M_t}^H (\mathbf{s}^T \otimes \mathbf{H}^*)) (\mathbf{q}_{s-t} - (\mathbf{s} \otimes \mathbf{H}^T) \mathbf{w}_{M_t})].$$
(32)

We set the gradient equal to $\mathbf{0} \in \mathbb{C}^{M_t}$ and calculate

$$-(\mathbf{s}^T \otimes \mathbf{H}^*)\mathbf{q}_{s-t} + (\mathbf{s}^T \otimes \mathbf{H}^*)(\mathbf{s} \otimes \mathbf{H}^T)\mathbf{w}_{M_t} = \mathbf{0}_{M_t \times 1}.$$
(33)

We solve (33) to obtain

$$\mathbf{w}_{M_t}^{opt} = inv[(\mathbf{s}^T \otimes \mathbf{H}^*)(\mathbf{s} \otimes \mathbf{H}^T)](\mathbf{s}^T \otimes \mathbf{H}^*)\mathbf{q}_{s-t}$$
(34)

where $(\mathbf{s}^T \otimes \mathbf{H}^*)(\mathbf{s} \otimes \mathbf{H}^T)$ is invertible if $rank(\mathbf{H}) \geq M_t$.

ACKNOWLEDGMENT

Distribution A. Approved for public release: Distribution unlimited: AFRL-2023-1770 on 12 Apr 2023.

REFERENCES

- [1] M. U. A. Siddiqui, F. Qamar, F. Ahmed, Q. N. Nguyen, and R. Hassan, "Interference management in 5G and beyond network: Requirements, challenges and future directions," *IEEE Access*, vol. 9, pp. 68932–68965, 2021
- [2] Y. Cao, T. Jiang, and Z. Han, "A survey of emerging M2M systems: Context, task, and objective," *IEEE Internet Things J.*, vol. 3, no. 6, pp. 1246–1258, Dec. 2016.
- [3] H. Han, Y. Li, W. Zhai, and L. Qian, "A grant-free random access scheme for M2M communication in massive MIMO systems," *IEEE Internet Things J.*, vol. 7, no. 4, pp. 3602–3613, Apr. 2020.
- [4] Z. Chen and D. Smith, "MmWave M2M networks: Improving delay performance of relaying," *IEEE Trans. Wireless Commun.*, vol. 20, no. 1, pp. 577–589, Jan. 2021.
- [5] L. Chettri and R. Bera, "A comprehensive survey on Internet of Things (IoT) toward 5G wireless systems," *IEEE Internet Things J.*, vol. 7, no. 1, pp. 16–32, Jan. 2020.
- [6] S. Naderi, D. B. D. Costa, and H. Arslan, "Channel randomness-based adaptive cyclic prefix selection for secure OFDM system," *IEEE Wireless Commun. Lett.*, vol. 11, no. 6, pp. 1220–1224, Jun. 2022.
- [7] S. Naderi, D. B. da Costa, and H. Arslan, "Joint random subcarrier selection and channel-based artificial signal design aided PLS," *IEEE Wireless Commun. Lett.*, vol. 9, no. 7, pp. 976–980, Jul. 2020.
- [8] H. Salman, S. Naderi, and H. Arslan, "Channel-dependent code allocation for downlink MC-CDMA system aided physical layer security," in *Proc. IEEE 95th Veh. Technol. Conference: (VTC-Spring)*, Helsinki, Finland, Jun. 2022, pp. 1–5.
- [9] Z. Li, M. A. Uusitalo, H. Shariatmadari, and B. Singh, "5G URLLC: Design challenges and system concepts," in *Proc. IEEE ISWCS*, Lisbon, Portugal, Aug. 2018, pp. 1–6.

- [10] K. Zhang, X. Xu, J. Zhang, B. Zhang, X. Tao, and Y. Zhang, "Dynamic multiconnectivity based joint scheduling of eMBB and uRLLC in 5G networks," *IEEE Syst. J.*, vol. 15, no. 1, pp. 1333–1343, Mar. 2021.
- [11] P. Popovski, K. F. Trillingsgaard, O. Simeone, and G. Durisi, "5G wireless network slicing for eMBB, URLLC, and mMTC: A communication-theoretic view," *IEEE Access*, vol. 6, pp. 55765–55779, 2018
- [12] S. Das and H. Viswanathan, "Interference mitigation through interference avoidance," in *Proc. Asilomar*, Pacific Grove, CA, Oct. 2006, pp. 1815–1819.
- [13] C. Rose, S. Ulukus, and R. D. Yates, "Wireless systems and interference avoidance," *IEEE Trans. Wireless Commun.*, vol. 1, no. 3, pp. 415–428, Jul. 2002.
- [14] G. Sklivanitis et al., "All-spectrum cognitive channelization around narrowband and wideband primary stations," in *Proc. IEEE GLOBECOM*, San Diego, CA, USA, Dec. 2015, pp. 1–7.
- [15] G. Sklivanitis et al., "Airborne cognitive networking: Design, development, and deployment," *IEEE Access*, vol. 6, pp. 47217–47239, 2018.
- [16] K. Tountas, G. Sklivanitis, D. A. Pados, and S. N. Batalama, "All-spectrum digital waveform design via bit flipping," in *Proc. IEEE GLOBECOM*, Abu Dhabi, UAE, Dec. 2018, pp. 1–6.
- [17] L. Ding, K. Gao, T. Melodia, S. N. Batalama, D. A. Pados, and J. D. Matyjas, "All-spectrum cognitive networking through joint distributed channelization and routing," *IEEE Trans. Wireless Commun.*, vol. 12, no. 11, pp. 5394–5405, Nov. 2013.
- [18] G. Sklivanitis, P. P. Markopoulos, S. N. Batalama, and D. A. Pados, "Sparse waveform design for all-spectrum channelization," in *Proc. IEEE ICASSP*, New Orleans, LA, USA, Mar. 2017, pp. 3764–3768.
- [19] K. Tountas, G. Sklivanitis, and D. A. Pados, "Directional spacetime waveform design for interference-avoiding MIMO configurations," in *Proc. Int. Workshop Antenna Technol. (iWAT)*, Miami, FL, USA, Mar. 2019, pp. 235–238.
- [20] K. Tountas, G. Sklivanitis, and D. A. Pados, "Dynamic joint PHY-MAC waveform design for IoT connectivity," in *Proc. IEEE Int. Conf. Acoust., Speech Signal Process. (ICASSP)*, Brighton, U.K., May 2019, pp. 8399–8403.
- [21] J. Molins-Benlliure et al., "Design of a MIMO 5G indoor base station antenna using unit cells," in *Proc. EuCAP*, Madrid, Spain, Mar. 2022, pp. 1–4.
- [22] J. Zhang, E. Björnson, M. Matthaiou, D. W. K. Ng, H. Yang, and D. J. Love, "Prospective multiple antenna technologies for beyond 5G," *IEEE J. Sel. Areas Commun.*, vol. 38, no. 8, pp. 1637–1660, Aug. 2020.
- [23] S. Mazokha et al., "Single-sample direction-of-arrival estimation for fast and robust 3D localization with real measurements from a massive MIMO system," in *Proc. IEEE ICASSP*, Rhodes Island, Greece, Jun. 2023, pp. 1–5.
- [24] Y. Takano, H.-J. Su, Y. Shiraishi, and M. Morii, "A spatial-temporal subspace-based compressive channel estimation technique in unknown interference MIMO channels," *IEEE Trans. Signal Process.*, vol. 68, pp. 300–313, 2020.
- [25] Y. Abdulkadir, O. Simpson, N. Nwanekezie, and Y. Sun, "Space-time opportunistic interference alignment in cognitive radio networks," in *Proc. IEEE Wireless Commun. Netw. Conf.*, Doha, Qatar, Apr. 2016, pp. 1–6.
- [26] R. A. Osman, S. N. Saleh, and Y. N. M. Saleh, "A novel interference avoidance based on a distributed deep learning model for 5G-enabled IoT," Sensors, vol. 21, no. 19, p. 6555, Sep. 2021.
- [27] X. Zhao, X. Zhang, S. Li, F. Jiang, and J. Peng, "A cooperative interference eliminated mechanism in MIMO systems," in *Proc. IEEE BigComp*, Shanghai, China, Jan. 2018, pp. 569–572.
- [28] S. Loyka, "On optimal signaling over Gaussian MIMO channels under interference constraints," in *Proc. IEEE Global Conf. Signal Inf. Process.* (GlobalSIP), Montreal, QC, Canada, Nov. 2017, pp. 220–223.
- [29] S. Loyka, "The capacity and optimal signaling for Gaussian MIMO channels under interference constraints," *IEEE Trans. Commun.*, vol. 68, no. 6, pp. 3386–3400, Jun. 2020.
- [30] M. Newinger and W. Utschick, "Interference shaping for sumrate maximization in cellular full-duplex MIMO networks," in *Proc. IEEE Globecom Workshops (GC Wkshps)*, Singapore, Dec. 2017, pp. 1–6.

- [31] Z. He, X. Huang, J. Zhong, and Y. Rong, "Transceiver design for interference MIMO relay systems with direct links," *IEEE Trans. Veh. Technol.*, vol. 66, no. 5, pp. 4476–4481, May 2017.
- [32] E. Björnson, Ö. T. Demir, and L. Sanguinetti, "A primer on near-field beamforming for arrays and reconfigurable intelligent surfaces," in *Proc. Asilomar Conf. Signals, Syst., Comp.*, Pacific Grove, CA, Oct. 2021, pp. 105–112.



Sanaz Naderi (Graduate Student Member, IEEE) received the B.S. and M.S. degrees in electrical engineering. She is currently pursuing the Ph.D. degree in electrical engineering with the Center for Connected Autonomy and AI (CA-AI), Department of Electrical Engineering and Computer Science, Florida Atlantic University, USA. Her research interests include the theory and development of wireless communication systems, physical layer security, interference avoidance, and waveform design.



Dimitris A. Pados (Senior Member, IEEE) received the Diploma degree in computer science and engineering from the University of Patras, Greece, and the Ph.D. degree in electrical engineering from the University of Virginia, Charlottesville, VA, USA. From 1997 to 2017, he was with the Department of Electrical Engineering, The State University of New York at Buffalo, as an Assistant Professor, an Associate Professor, a Professor, and a Clifford C. Furnas Chair Professor of Electrical Engineering. He was the Associate Chair and the Chair of the Department

of Electrical Engineering. He was elected as an University Faculty Senator four times and a Faculty Senate Executive Committee for two terms. In 2017, he joined Florida Atlantic University, Boca Raton, FL, USA, as the Schmidt Eminent Scholar Professor of Engineering and Computer Science and a fellow of the Institute for Sensing and Embedded Network Systems Engineering (I-SENSE). He is currently the Founding Director of the FAU Center for Connected Autonomy and Artificial Intelligence (https://ca-ai.fau.edu/). He is also the Acting Executive Director of FAU I-SENSE. He is a member of the IEEE Communications Society, IEEE Signal Processing Society, IEEE Information Theory Society, and IEEE Computational Intelligence Society. He served as an Associate Editor for the IEEE SIGNAL PROCESSING LET-TERS and IEEE TRANSACTIONS ON NEURAL NETWORKS. Several articles, that he coauthored with his students received IEEE conferences and journal article awards, among which notably the 2003 IEEE TRANSACTIONS ON NEURAL NETWORKS Outstanding Paper Award for groundbreaking work on overfitting, generalization error, and randomly expanded training sets. He was a recipient of the 2009 SUNY-Wide Chancellor's Award for Excellence in Teaching and the 2011 University at Buffalo Exceptional Scholar-Sustained Achievement Award. He was presented with the 2021 Florida Atlantic Research & Development Authority Distinguished Researcher Award, Boca Raton, the 2022 Florida Atlantic University Researcher of the Year Award, and the 2023 National John J. Guarrera Engineering Educator of the Year Award. He has served as a principal or co-principal investigator on more than 50 federal (NSF and DoD) and private-sector research grants of about \$20M in aggregate and has been author/coauthor of 250 journals and conference proceedings in predominantly IEEE venues. Technical contributions from his team include small-sample-support adaptive MMSE filtering (auxiliaryvector filters), optimal multiple-access code sets (Karystinos-Pados bounds and designs), and L1-norm principal-component analysis (optimal algorithms for exact L1-norm PCA).



George Sklivanitis (Member, IEEE) is currently the Schmidt Research Associate Professor in electrical engineering and computer science with Florida Atlantic University, a Faculty Founding Member of the FAU Center for Connected Autonomy and AI (ca-ai.fau.edu), and a Faculty Fellow with the FAU Institute for Sensing and Embedded Network Systems Engineering (I-SENSE). His research focuses on modeling, optimization and experimental evaluation of advanced wireless communication systems and autonomy in challenging, and congested (and

sometimes contested) communication environments. He has made leading contributions in software-defined radio testbeds for cognitive wireless mesh networking. In 2021, he was recognized by the Economist as one of the three winners of the 2021 World Ocean Initiative's Ocean Changemakers Challenge. In 2014, he ranked first among all U.S. Universities in the Nutaq Software-defined Radio Academic U.S. National Contest. He is a member of the ACM, SPIE, IEEE Communications Society, IEEE Signal Processing Society, and IEEE Oceanic Engineering Society. Since 2017, he has been serving as the Co-Organizer and a Technical Program Committee Co-Chair for the IEEE Workshop on Wireless Communications and Networking in Extreme Environments (WCNEE). He has won several teaching and research awards, including Best Paper Award Finalist in the 15th IEEE International Workshop on Antenna Technology (iWAT-2019), 2017 SUNY Chancellor's Award, Best Demo Award in the 10th ACM International Conference on Underwater Networks and Systems (WUWNet-2015), and 2015 SUNY Buffalo Graduate Student Award for Excellence in Teaching. His research at FAU is funded by NSF, AFOSR, AFRL, ARO, PAR Government, NATO CMRE, and the Schmidt Family Foundation.



Elizabeth Serena Bentley (Member, IEEE) received the B.S. degree in electrical engineering from Cornell University, the M.S. degree in electrical engineering from Lehigh University, and the Ph.D. degree in electrical engineering from University at Buffalo. She is currently a Senior Electrical Engineer with the Information Directorate of the Air Force Research Laboratory, Rome, NY, USA. Her research interests include cross-layer optimization, directional networking, swarm networking, and waveform design.

Joseph Suprenant, photograph and biography not available at the time of publication.



Michael J. Medley (Senior Member, IEEE) received the Ph.D. degree in electrical engineering from the Rensselaer Polytechnic Institute, Troy, NY, USA, in 1995. In 2002, he joined as a Faculty Member of the State University of New York Polytechnic Institute, Utica, NY, USA, where he is currently an Associate Professor in electrical and computer engineering. Since 1991, he has been with the United States Air Force Research Laboratory as a Communications and Signal Processing Research Engineer in adaptive interference suppression, spread spec-

trum waveform design, spectrum management, covert messaging, terahertz communications, and cross-layer network communications.